

High particulate nitrate formation via N_2O_5 uptake in a chemically reactive layer aloft during wintertime in Beijing

Haichao Wang¹, Keding Lu^{1*}, Xiaorui Chen¹, Qindan Zhu^{1, #}, Zhijun Wu¹, Yusheng Wu¹, Kang Sun²

¹State Key Joint Laboratory of Environmental Simulation and Pollution Control, College of Environmental Sciences and Engineering, Peking University, Beijing, China

²China National Environmental Monitoring Centre, Beijing, China

[#]Now at the Department of Chemistry, University of California, Berkeley, CA 94720, USA

*Correspondence to: Keding Lu (k.lu@pku.edu.cn)

Abstract.

Particulate nitrate (pNO_3^-) is a dominant component of secondary aerosols in urban areas. Therefore, it is critical to explore its formation mechanism to assist with the planning of haze abatement strategies. Simultaneous ground-based and tower-based measurements of NO_x and O_3 were conducted during a winter heavy-haze episode (December 18 to 20, 2016) in urban Beijing, China. We found that pNO_3^- formation via N_2O_5 heterogeneous uptake was negligible at ground level, owing to the presence of high NO concentrations, which limited the production of N_2O_5 . In contrast, the contribution from N_2O_5 uptake was larger at higher altitudes (e.g., > 150 m), which was supported by the low total oxidant ($\text{NO}_2 + \text{O}_3$) level at higher altitudes than at ground level. Modeling results show that the nighttime integrated production of pNO_3^- for the higher altitude air mass above urban Beijing was estimated to be $50 \mu\text{g m}^{-3}$ and enhanced the surface-layer pNO_3^- the next morning significantly by $28 \mu\text{g m}^{-3}$ through vertical mixing. The overnight NO_x loss via NO_3 - N_2O_5 chemistry was efficient aloft ($> 50\%$). The nocturnal NO_x loss was easily maximized once the N_2O_5 uptake coefficient was over 2×10^{-3} on polluted days in wintertime. These results highlight that pNO_3^-

formation via N_2O_5 heterogeneous hydrolysis in higher altitude air masses could be an important source for haze formation in the urban airshed during wintertime. Accurately describing the formation and development of reactive air masses aloft is a critical task for improving current chemical transport models.

1. Introduction

Winter particulate matter (PM) pollution events occur frequently in China and have drawn widespread and sustained attention in recent years (Guo et al., 2014; Zhang et al., 2015; Huang et al., 2014; Wang G et al., 2016). PM pollution reduces visibility (Lei and Wuebbles, 2013) and has harmful effects on public health (Cao et al., 2012). Particulate nitrate (pNO_3^-) is an important component of secondary inorganic aerosols and contributes 15%–40% of the $\text{PM}_{2.5}$ mass concentration in China (Sun et al., 2013, 2015a, 2015b; Chen et al., 2015; Zheng et al., 2015; Wen et al., 2015). The main atmospheric pathways of nitrate formation are (1) the reaction of OH with NO_2 and (2) N_2O_5 heterogeneous hydrolysis (Seinfeld and Pandis, 2006). The reaction of OH with NO_2 is a daytime pathway, as OH is severely limited at night, and N_2O_5 uptake is a nighttime pathway, as NO_3 and N_2O_5 are easily photo-labile.

Particulate nitrate formation via N_2O_5 heterogeneous hydrolysis in summer in north China was proved efficient by ground-based observation (Wang H et al., 2017b; Wang Z et al., 2017) and found comparable to or even higher than the daytime formation. Several studies showed that N_2O_5 hydrolysis is responsible for nocturnal pNO_3^- enhancement in summer Beijing (Pathak et al., 2009, 2011; Wang H et al., 2017a). Although pNO_3^- formation via N_2O_5 uptake is significant in summertime, the importance of this pathway in wintertime is not well characterized. Many differences in N_2O_5 chemistry exist between winter and summer. First, as the key precursor of NO_3 and N_2O_5 , O_3 has a much lower concentration in winter than in summer, owing to the short daytime length and weak solar radiation. Second, colder temperatures and high NO_2 levels favor partitioning towards N_2O_5 . Third, nighttime lasts much longer in winter, making N_2O_5 heterogeneous hydrolysis potentially more important in pNO_3^-

formation. Finally, the N_2O_5 uptake coefficient, the most important parameter in N_2O_5 heterogeneous hydrolysis, is likely very different from that in summer. This is because the properties of aerosol particles (e.g., organic compounds, particulate nitrate, liquid water contents, solubility, and viscosity) and meteorological conditions (e.g., temperature and relative humidity) differ between summer and winter (Chen et al., 2015; Zhang et al., 2007). These effects would result in large variations in the N_2O_5 uptake coefficient (Wahner et al., 1998; Mentel et al., 1999; Kane et al., 2001; Hallquist et al., 2003; Thornton et al., 2003; Bertram and Thornton, 2009; Wagner et al., 2013; Grzinic et al., 2015). Several parameterization methods have been unsuccessful in predicting N_2O_5 uptake coefficient accurately (Chang et al., 2011; Chang et al., 2016).

In addition to the seasonal differences in pNO_3^- formation via N_2O_5 uptake, modeling and field studies showed greater levels of NO_3 and N_2O_5 at higher altitudes within the nocturnal boundary layer (NBL), owing to the stratification of surface NO and volatile organic compounds (VOCs) emissions, which lead to gradients in the loss rates for these compounds as a function of altitude (e.g., Brown et al., 2007; Geyer and Stutz, 2004; Stutz et al., 2004). The pNO_3^- formation via N_2O_5 uptake contributes to the gradients in the compounds percentage and size distribution of the particle (Ferrero et al., 2010; 2012). On nights when NO_3 production in the surface layer is negligible owing to high NO emissions, N_2O_5 uptake can still be active aloft without NO titration. The N_2O_5 uptake aloft leads to elevated pNO_3^- formation in the upper layer as well as effective NO_x removal (Watson et al., 2002; S. G. Brown et al., 2006; Lurmann et al., 2006; Pusede et al., 2016; Baasandorj et al., 2017). Field observations at high altitude sites of Kleiner Feldberg, Germany (Crowley et al., 2010a); the London British Telecommunications tower, UK (Benton et al., 2010); and Boulder, CO, USA (Wagner et al., 2013) showed the elevated N_2O_5 concentrations aloft. Model studies showed that pNO_3^- varied at different heights and stressed the importance of the heterogeneous formation mechanism (Kim et al., 2014; Ying, 2011; Su et al., 2017). The mass fraction and concentration of pNO_3^- in Beijing was reported higher aloft (260 m) than at the ground level in Beijing (Chan et al., 2005; Sun et al., 2015b),

which was explained by favorable gas–particle partitioning aloft under lower temperature conditions. The active nighttime chemistry in the upper level plays an important role in surface PM pollution through mixing and dispersing within the planet boundary layer (PBL) (Prabhakar et al., 2017), especially in valley terrain regions coupled with meteorological processes (Baasandorj et al., 2017; Green et al., 2015).

To explore the possible sources of pNO_3^- and the dependence of its formation on altitude in wintertime in Beijing, we conducted vertical profile measurements of NO , NO_2 , and O_3 with a tower platform in combination with simultaneous ground measurements of these parameters in urban Beijing. A box model was used to investigate the reaction rate of N_2O_5 heterogeneous hydrolysis and its impact on pNO_3^- formation at different altitudes during a heavy haze episode over urban Beijing. Additionally, the dependence of NO_x removal and pNO_3^- formation on the N_2O_5 uptake coefficient was probed.

2. Methods

2.1 Field measurement

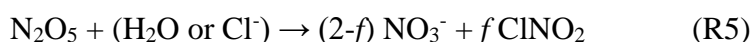
Ground measurements (15 m above the ground) were carried out on the campus of Peking University (PKU; 39°59'21"N, 116°18'25"E) in Beijing, China. The vertical measurements were conducted at the Institute of Atmospheric Physics (IAP), Chinese Academy of Sciences (39°58'28"N, 116°22'16"E). The IAP site is within 4 km of the PKU site. The locations of the PKU and IAP sites are shown in Fig. 1. At the PKU site, dry-state mass concentration of $\text{PM}_{2.5}$ was measured using a TEOM 1400A analyzer. NO_x was measured via a chemiluminescence analyzer (Thermo Scientific, TE-42i-TR), and O_3 was measured with a UV photometric O_3 analyzer (Thermo Scientific, TE-49i). Dry-state particle number and size distribution (PNSD) was measured from 0.01 to 0.7 μm with a Scanning Mobility Particle Sizer (SMPS; TSI Inc. 3010). The instrumental parameters are summarized in Table S1. The data were collected from December 16 to 22, 2016. Additionally, relative humidity (RH),

temperature (T), and wind direction and speed data were available during the measurement period.

Vertical profile measurements were conducted from December 18 to 20, 2016, from the tower-based platform (maximum height: 325 m) on the IAP campus. The NO_x and O_3 instruments were installed aboard a movable cabin on the tower. NO_x and O_3 were measured with two low-power, lightweight instruments (Model 405 nm and Model 106-L, 2B Technologies, USA). The Model 405 nm instrument measures NO_2 directly based on the absorbance at 405 nm, and NO is measured by adding excess O_3 (conversion efficiency $\sim 100\%$). The limit of detection of both NO and NO_2 is 1 part per billion volume (ppbv), with an accuracy of 2 ppbv or 2% of the reading, and the time resolution is 10 s (Birks et al., 2018). The Model 106-L instrument measures O_3 based on the absorbance at 254 nm, with a precision of 1 ppbv, or 2% of the reading, and a limit of detection of 3 ppbv. NO_x calibration was performed in the lab using a gas calibrator (TE-146i, Thermo Electron, USA) associated with a NO standard (9.8 ppmv). The O_3 calibration was done with an O_3 calibrator (TE 49i-PS), which was traceable to NIST (National Institute of Standards and Technology) standards annually. Before the campaign, the NO_x monitor was compared with a Cavity Attenuated Phase Shift (CAPS) Particle Light Extinction Monitor, and the O_3 monitor was compared to a commercial O_3 analyzer (TE-49i, Thermo Electron, USA). Good agreement was found between the portable instruments and the conventional monitors. Height information was retrieved via the observed atmospheric pressure measured by the Model 405 nm instrument. The cabin ascended and descended at a rate of 10 m min^{-1} , with a height limit of 260 m during the daytime and 240 m at night. The cabin stopped after reaching the peak, and parameters were measured continually during the last 10 min of each cycle. One vertical cycle lasted for approximately 1 h. We measured two cycles per day, one in the morning and the other in the evening, with six measurement cycles conducted in total during the campaign.

2.2 Box model simulation

A box model was used to model the NO₃ and N₂O₅ mixing ratios and the nitrate formation potential in vertical scale at the IAP site. A simple chemical mechanism (see R1–R5) was used to model the nighttime NO₃ and N₂O₅ chemistry under NO free-air-mass conditions. Physical mixing, dilution, deposition, or interruption during the transport of the air mass was not considered. Here, f represents the ClNO₂ yield from N₂O₅ uptake. Homogeneous hydrolysis of N₂O₅ and NO₃ heterogeneous uptake reaction were neglected in this analysis because of the low level of absolute humidity and the extremely low NO₃ concentration during wintertime (Brown and Stutz, 2012). The corresponding rate constants of R1–R3 are those reported by Sander et al. (2011).



Following the work of Wagner et al. (2013), the box model can be solved using six equations (Eqs. 1–6). In the framework, O₃ is only lost via the reaction of NO₂ + O₃ and the change in the O₃ concentration can be expressed as Eq. 1. Eq. 2 can express the losses of NO₂. Here, the $s(t)$ is between 0 and 1 and expressed as Eq. 5. The $s(t)$ favors 0 when direct loss of NO₃ dominates and favors 1 when N₂O₅ uptake dominates NO₃ loss. The model calculation had two steps. The first step was to calculate the mixing ratio of NO₂ and O₃ at time zero (herein designated as sunset). According to Eqs. 1 and 2, the initial NO₂ ($t=0$) and O₃ ($t=0$) concentrations can then be integrated backward in time starting with the measured concentrations of NO₂ and O₃ at each height. During the pollution period in winter in Beijing (NO₂ = 45 ppbv, Temperature = 273 K, $S_a = 3000 \mu\text{m}^2 \text{cm}^{-3}$), the ratio of N₂O₅ to NO₃ is large enough, i.e., 450. The pseudo-first-order loss rate of N₂O₅ heterogeneous uptake will be $1 \times 10^{-3} \text{ s}^{-1}$, with a N₂O₅ uptake coefficient of 5×10^{-3} . N₂O₅ uptake would contribute an NO₃ loss rate of 0.4 s^{-1} , which is much higher than the direct NO₃ loss through the reaction of NO₃ with VOCs, even with the k_{NO_3} set to a high value of 0.02 s^{-1} . Therefore, N₂O₅ uptake was proposed to be dominantly responsible for the NO₃ loss and the initial $s(t)$

was set to 1. Eq. 3 can describe the sum concentration of NO_3 and N_2O_5 . Assuming the equilibrium between NO_3 and N_2O_5 is maintained after a period, based on the temperature-dependent equilibrium rate constant (k_{eq}) and the modeled NO_2 at a certain time, Eq. 4 can be used to determine the ratio of N_2O_5 to NO_3 . Combined, Eqs. 1–4 allow for the calculation of NO_3 and N_2O_5 concentrations considering stable NO_3 and N_2O_5 loss rate constants (k_{NO_3} and $k_{\text{N}_2\text{O}_5}$, respectively). In the second step, a new $s(t)$ was calculated using the data from the first step (Eq. 5), new initial NO_2 and O_3 concentrations were then approximated, and NO_3 and N_2O_5 values were derived using the same method as used in the first step. This process was repeated until the difference between the two $s(t)$ values was less than 0.005. The number of adjustments to a new $s(t)$ could not be calculated more than 10 times. Otherwise, the calculating process would become non-convergent.

The modeled N_2O_5 concentrations and given $k_{\text{N}_2\text{O}_5}$ were then used to estimate pNO_3^- formation. The HNO_3 produced in R4 was not considered because many of the products are organic nitrates (Brown and Stutz, 2012). Here, k_{NO_3} and $k_{\text{N}_2\text{O}_5}$ denote the pseudo-first-order reaction rate constants of the total NO_3 reactivity caused by ambient VOCs and N_2O_5 heterogeneous uptake, respectively. $k_{\text{N}_2\text{O}_5}$ is given in Eq. 6. S_a is the aerosol surface area, C is the mean molecular speed of N_2O_5 , and $\gamma_{\text{N}_2\text{O}_5}$ is the N_2O_5 uptake coefficient. Sunset and sunrise times during the measurements were 16:55 and 07:30 (Chinese National Standard Time, CNST), and the model was run from sunset to sunrise, with the running time set to 14.5 h.

$$\frac{d[\text{O}_3]}{dt} = -k_{\text{NO}_2+\text{O}_3}[\text{O}_3][\text{NO}_2] \quad (1)$$

$$\frac{d[\text{NO}_2]}{dt} = -(1 + s(t)) \times k_{\text{NO}_2+\text{O}_3}[\text{O}_3][\text{NO}_2] \quad (2)$$

$$\frac{d[\text{NO}_3+\text{N}_2\text{O}_5]}{dt} = k_{\text{NO}_2+\text{O}_3}[\text{O}_3][\text{NO}_2] - k_{\text{N}_2\text{O}_5}[\text{N}_2\text{O}_5] - k_{\text{NO}_3}[\text{NO}_3] \quad (3)$$

$$\frac{[\text{N}_2\text{O}_5]}{[\text{NO}_3]} = k_{\text{eq}}[\text{NO}_2] \quad (4)$$

$$s(t) = \frac{\int_0^t k_{\text{N}_2\text{O}_5}[\text{N}_2\text{O}_5]dt + [\text{N}_2\text{O}_5]_t}{[\text{O}_3](0) - [\text{O}_3](t)} \quad (5)$$

$$k_{\text{N}_2\text{O}_5} = \frac{C \times S_a \times \gamma_{\text{N}_2\text{O}_5}}{4} \quad (6)$$

Dry-state S_a at the PKU site was calculated based on the PNSD measurement, which was corrected to ambient (wet) S_a for particle hygroscopicity via a growth factor (Liu et al., 2013). The uncertainty of the wet S_a was estimated to be ~30%, which was associated with the error from dry PNSD measurement (~20%) and the growth factor (~20%). Nighttime averaged S_a on the night of December 19 was about $3000 \mu\text{m}^2 \text{cm}^{-3}$. PM measurements at the National Monitoring Sites proved this heavy haze pollution episode was a typical regional event (Fig. S1). Furthermore, synchronous study on the night of December 19, 2016, showed small variation in the vertical particle number concentration, with a boundary layer height of 340 m (Zhong et al., 2017). Therefore, the S_a measured at the PKU site can represent the urban Beijing conditions in horizontal and vertical scale (< 340 m). Although the PNSD information for particles larger than $0.7 \mu\text{m}$ was not valid during the study period, the particles smaller than $0.7 \mu\text{m}$ dominated more than 95% of the aerosol surface area in a subsequent pollution episode (01/01/2017 to 01/07/2017), and similar results also were reported in other studies (e.g., Crowley et al., 2010a; Wang et al., 2018). The possible lower bias of S_a (5%) only led to a small overestimation of N_2O_5 , i.e., 3.6%–4.2%, and an underestimation of pNO_3^- of 0.2%–2.5% when $\gamma_{\text{N}_2\text{O}_5}$ varied from 1×10^{-3} to 0.05.

The N_2O_5 uptake coefficient and ClNO_2 yield are key parameters in the estimation of pNO_3^- formation (Thornton et al., 2010; Riedel et al., 2013; Wagner et al., 2013; Phillips et al., 2016). Wagner et al. (2013) shows the significant pNO_3^- suppression of N_2O_5 uptake aloft in the wintertime in Denver, CO, USA, the uptake coefficient is 0.005 when the percentage of pNO_3^- in the $\text{PM}_{2.5}$ mass concentration is 40%. As the proportion of nitrate in the particle mass concentration is similarly high in North China during wintertime (Sun et al., 2013, 2015a; Chen et al., 2015; Zheng et al., 2015; Wen et al., 2015), herein we fixed the uptake coefficient to 0.005 for the base model initial input. Because the model input of ClNO_2 yield only affects the value of produced pNO_3^- concentration and would not change the modeled N_2O_5 concentration,

we set the initial f_{CINO_2} to zero. The average value of k_{NO_3} of about 0.011 s^{-1} in summer Beijing was calculated in a previous work, with BVOCs contributing significantly (Wang H et al., 2017a; Wang et al., 2018). The intensity of biogenic VOCs emissions decreased in wintertime, owing to the lower temperature and weak solar radiation, thus the k_{NO_3} should be smaller than it is in summer. In this work, the model input k_{NO_3} was set to a relatively high value of 0.02 s^{-1} (equivalent to 0.2 ppbv isoprene + $40 \text{ parts per trillion volume (pptv)}$ monoterpene + 1.0 ppbv cis-2-butene), to constrain the impact of N_2O_5 uptake in the model. A series of sensitivity tests was conducted to study the uncertainties of the model simulation, and the detailed test sets are listed in Table 1, included the test of N_2O_5 uptake coefficient and k_{NO_3} . The $\gamma_{\text{N}_2\text{O}_5}$ sensitivity tests were set from 0.001 to 0.05, and the k_{NO_3} tests were set to 0.001 s^{-1} , 0.01 s^{-1} , and 0.1 s^{-1} .

3. Results and discussion

3.1 Ground-based observations.

A severe winter PM pollution event lasted from December 16 to 22, 2016, in Beijing. Figure 2a shows the time series of $\text{PM}_{2.5}$ and other relevant parameters based on ground measurements at the PKU site. The mass concentration of $\text{PM}_{2.5}$ began to increase from December 16, reaching $480 \mu\text{g m}^{-3}$ on December 20. A fast PM growth event was captured, with an overall increment of $100 \mu\text{g m}^{-3}$ on the night of December 19 (Fig. 2a). Throughout the pollution episode, the meteorological conditions included high RH ($50\% \pm 16\%$) and low temperature ($2 \pm 3 \text{ }^\circ\text{C}$). The slow surface wind speed ($< 3 \text{ m s}^{-1}$) implied the atmosphere was stable (Fig. 2c, d). The daytime O_3 concentration was low, owing to high NO emission and weak solar radiation. After sunset, O_3 at surface layer was rapidly titrated to zero by the elevated NO. The presence of high NO concentrations would have strongly suppressed the concentration of NO_3 , further suppressing N_2O_5 near the ground. Figure 2b depicts the high amounts of NO and NO_2 that were observed at ground level during the PM pollution episode, suggesting that pNO_3^- production via N_2O_5 uptake was not important near the ground during the winter haze episode.

259

260 **3.2 Tower observations.**

261 Six vertical measurements of the total oxidants ($O_x = O_3 + NO_2$) below 50 m were
262 consistent with those measured at ground level and are shown in Fig. S2, confirming
263 that the two sites are comparable. On the night of December 20 (Fig. 3a), the NO_2 and
264 NO from 0–240 m were abundant and conservative around 21:00, with concentrations
265 of 80 ppbv and 100 ppbv, respectively. The O_3 concentrations remained zero during
266 the nighttime (Fig. 3b). The vertical profile on December 20 suggests that at least
267 below 240 m, the N_2O_5 chemistry was not important, which is consistent with the
268 results at ground level as mentioned above. The case on the night of December 18 was
269 similar to that on the night of December 20, whereas the vertical profile on December
270 19 was not similar to that on December 20. Figure 4a shows the vertical profiles
271 around 21:00 on December 19; NO was abundant from the ground to 100 m, then
272 gradually decreased to zero from 100 m to 150 m, and remained at zero above 150 m.
273 The observed NO_2 concentration was 85 ± 2 ppbv below 100 m, which gradually
274 decreased from 100 m to 150 m, and was 50 ± 2 ppbv from 150 m to 240 m. The
275 observed O_3 concentrations below 150 m were below the instrumental limit of
276 detection (Fig. 4b). Above 150 m, the O_3 concentration was 20 ± 2 ppbv,
277 corresponding to the greatly diminished NO concentration. With respect to O_x , the
278 mixing ratio of O_x was 85 ± 2 ppbv at lower altitudes, whereas the O_x concentration at
279 higher altitudes was 15 ppbv lower than that at lower altitudes (Fig. 4b). The O_x
280 missing from the higher altitude air mass indicated an additional nocturnal removal of
281 O_x aloft.

282 Figure 5 depicts the vertical profiles of NO_x , O_3 , and O_x at 09:30 on the morning of
283 December 20, which have similar features to those observed at 21:00 on December 19.
284 The vertical profiles suggested stratification still existed at that time. The amount of
285 O_x missing aloft in the morning increased to 25 ppbv at 240–260 m, demonstrating
286 that an additional 25 ppbv of O_x was removed or converted to other compounds at
287 higher altitudes than at the surface layer during the night from December 19 to 20.

Figure S3 shows the vertical profiles of NO, NO₂, O₃, and O_x at ~12:00 on December 18, when solar radiation was strong enough to mix the trace gases well in the vertical direction. NO_x and O₃ were found to be well mixed indeed, with small variation from the ground level to 260 m.

3.3 Particulate nitrate formation aloft.

N₂O₅ uptake is one of the two most important pathways of ambient NO_x loss and an important pathway of pNO₃⁻ formation (Wagner et al., 2013; Stutz et al., 2010; Tsai et al., 2014). At higher altitudes (e.g., > 150 m), NO₃ and N₂O₅ chemistry can be initiated in the co-presence of high NO₂ and significant O₃ levels. Therefore, N₂O₅ uptake could represent a plausible explanation for the O_x observed missing from the higher altitude air masses on the night of December 19. To explore this phenomenon, a time-step box model was used to simulate the NO₃ and N₂O₅ chemistry based on the observed vertical profiles of NO₂ and O₃ on the night of December 19.

In the base case, the average initial NO₂ and O₃ levels above 150 m at sunset were about 61 ± 3 ppbv and 27 ± 6 ppbv, respectively. The measured NO₂ concentration at the PKU site at sunset (local time, 16:55) was 61 ppbv and showed good consistency with the model result. The modeled N₂O₅ concentration was zero below 150 m, as the high level of NO made for quick consumption of the NO₃ formed. In contrast, the modeled N₂O₅ concentrations at 21:00 above 150 m were in the range of 400–600 pptv (Fig. 6a). Particulate NO₃⁻ accumulation via N₂O₅ heterogeneous uptake from sunset to the measurement time, which can be calculated using Eq. 7, was significant above 150 m, with a maximum of 24 µg m⁻³ 4.5 hours after sunset (Fig. 6b).

$$\sum \text{pNO}_3^- = \int_0^t (2 - f) \cdot k_{\text{N}_2\text{O}_5} \cdot [\text{N}_2\text{O}_5] dt \quad (7)$$

The box model enabled the analysis of the integrated pNO₃⁻ and ClNO₂ via N₂O₅ uptake throughout the night. As shown in Fig. 6c, the modeled integrated pNO₃⁻ went as high as 50 µg m⁻³. The integrated pNO₃⁻ at sunrise was equal to the loss of 27 ppbv O_x, showing good agreement with the observed O_x missing aloft in the morning hours.

During the nighttime, the pNO_3^- formed aloft via N_2O_5 uptake led to the much higher particle nitrate concentration than that in the surface layer, which has been reported in many field observations (Watson et al., 2002; S. G. Brown et al., 2006; Lurmann et al., 2006; Ferrero et al., 2012; Sun et al., 2015b). The elevated pNO_3^- aloft was well dispersed through vertical mixing and enhanced the surface-layer PM concentration; this phenomenon was also observed in previous studies (Watson et al., 2002; S. G. Brown et al., 2006; Lurmann et al., 2006; Prabhakar et al., 2017). Zhong et al. (2017) showed that the NBL and PBL both were at 340 m from December 19 to 20, 2016 in Beijing. Daytime vertical downward transportation was helpful in mixing the air mass within the PBL. Assuming the newly formed pNO_3^- aloft from 150 m to 340 m is $50 \mu\text{g m}^{-3}$ during the nighttime and well mixed within the PBL by the next morning, the enhancement to the surface layer (ΔpNO_3^-) can be simplified to the calculation in Eq. 8 as following:

$$\Delta\text{pNO}_3 = \frac{\int_0^{150} P(\text{pNO}_3) dH + \int_{150}^{340} P(\text{pNO}_3) dH}{340} \quad (8)$$

Here, $P(\text{pNO}_3^-)$ is the integral production of pNO_3^- and H represents height. Owing to high NO below 150 m, the pNO_3^- formation via N_2O_5 uptake was zero. The enhancement of pNO_3^- from 150 m to 340 m was calculated as $28 \mu\text{g m}^{-3}$, which is in good agreement with the observed PM peak in the morning on December 20, with PM enhancement of $\sim 60 \mu\text{g m}^{-3}$. The result demonstrated that the nocturnal N_2O_5 uptake aloft and downward transportation were critical for understanding the PM growth process.

3.4 Sensitivity studies.

Previous studies have emphasized that the N_2O_5 uptake coefficient varies greatly (0.001–0.1) in different ambient conditions (Chang et al., 2011; Brown and Stutz, 2012; Wang H et al., 2016), which is the main source of uncertainties in this model. In the present research, sensitivity studies showed the modeled N_2O_5 concentration dropping from 3 ppbv to 60 pptv when the N_2O_5 uptake coefficients increased from

0.001 to 0.05 (Fig. 6a), as the N_2O_5 concentration is very sensitive to the loss from heterogeneous reactions. Compared to the base case, the accumulated pNO_3^- was evidently lower at $\gamma = 0.001$ with the accumulated pNO_3^- of $44 \mu\text{g m}^{-3}$, thus the low N_2O_5 uptake coefficient condition corresponded to several kinds of aerosols, such as secondary organic aerosols (Gross et al., 2009), humic acids (Badger et al., 2006), and certain solid aerosols (Gross et al., 2008). When the N_2O_5 uptake coefficient increased from 0.005 to 0.05 (Fig. 6b, c), the increase in integral pNO_3^- was negligible. This indicates that the conversion capacity of N_2O_5 uptake to pNO_3^- was almost maximized at certain ClNO_2 yield. The conversion of NO_x to nitrate was not limited by the N_2O_5 heterogeneous reaction rate, but by the formation of NO_3 via the reaction of NO_2 with O_3 during the polluted night.

For describing the nocturnal NO_x removal capacity and pNO_3^- formation via NO_3 and N_2O_5 chemistry, the overnight NO_x loss efficiency (ε) was calculated using Eq. 9.

$$\varepsilon = \frac{\int_0^t 2 \times k_{\text{N}_2\text{O}_5} [\text{N}_2\text{O}_5] dt + \int_0^t k_{\text{NO}_3} [\text{NO}_3] dt}{[\text{NO}_2](0)} \quad (9)$$

The case modeled typical winter haze pollution conditions in Beijing from sunset to sunrise, with the initial model values of NO_2 and O_3 set to 60 ppbv and 30 ppbv, respectively. S_a was set to $3000 \mu\text{m}^2 \text{cm}^{-3}$, the ClNO_2 yield was zero, and k_{NO_3} was 0.02 s^{-1} . The reaction time was set to 14.5 h to represent an overnight period in wintertime. The consumed NO_3 by the reaction with VOCs and N_2O_5 by uptake reaction were regarded as valid NO_x loss. Figure 7 shows the dependence of the overnight NO_x loss efficiency on N_2O_5 uptake, as it varied from 1×10^{-5} to 0.1. This is an increase from 20% to 56%, with increasing $\gamma_{\text{N}_2\text{O}_5}$, and the maximum NO_x loss efficiency was very large, as was addressed by Chang et al. (2011). The ceiling of overnight NO_x loss via NO_3 - N_2O_5 was fixed when all the NO_x loss was through N_2O_5 uptake, which is limited by the reaction time and the formation rate of NO_3 (R1). In this case, the N_2O_5 uptake was contributed about 90% of the overnight NO_x loss (50.4%) when $\gamma_{\text{N}_2\text{O}_5}$ was equal to 0.002. When $\gamma_{\text{N}_2\text{O}_5}$ was less than 2×10^{-3} , NO_x removal increased rapidly with the increasing of $\gamma_{\text{N}_2\text{O}_5}$, which was defined as the $\gamma_{\text{N}_2\text{O}_5}$ -sensitive region. When $\gamma_{\text{N}_2\text{O}_5} \geq 2 \times 10^{-3}$, the contribution of N_2O_5 uptake to NO_x

loss was over 90% and became insensitive, this region was defined as the $\gamma_{\text{N}_2\text{O}_5}$ -insensitive region. According to Eqs. 3 and 5, higher aerosol surface concentration and NO_x and lower k_{NO_3} and temperature would further increase the insensitivity region with lower $\gamma_{\text{N}_2\text{O}_5}$ value and allow the N_2O_5 uptake to be more easily located in the $\gamma_{\text{N}_2\text{O}_5}$ -insensitive region. Here, the critical value of the N_2O_5 uptake coefficient (2×10^{-3}) was relatively low compared to that recommended by the IUPAC (International Union of Pure and Applied Chemistry) on the surface of mineral dust (0.013, 290–300 K) (Crowley et al., 2010b) or determined in many field experiments (e.g., S. S. Brown et al., 2006; 2009; Wagner et al., 2013; Morgan et al., 2015; Phillips et al., 2016; Wang Z et al., 2017; Brown et al., 2016; Wang H et al., 2017b; Wang X et al., 2017). This suggests that the NO_x loss and pNO_3^- formation via N_2O_5 uptake were easily maximized in the pollution episode, further worsening the PM pollution.

In the base case, the modeled pNO_3^- formation via N_2O_5 uptake was an upper limit result, as the ClNO_2 yield was set to zero. High coal combustion emitted chloride into the atmosphere of Beijing during the heating period (Sun et al., 2013), like the emissions from power plants in north China. This enhanced anthropogenic chloride provides abundant chloride-containing aerosols to form ClNO_2 via N_2O_5 uptake aloft, implying that significant ClNO_2 formed in the upper layer of the NBL (Tham et al., 2016; Wang Z et al., 2017). Assuming the ClNO_2 yield is the average value of 0.28 determined at high altitude in north China (Wang Z et al., 2017), the pNO_3^- produced throughout the night will have decreased by $7 \mu\text{g m}^{-3}$. The ClNO_2 formation aloft throughout the night reached 2.5 ppbv, which is comparable with that observed in field measurement in north China (Tham et al., 2016; Wang Z et al., 2017; Wang X et al., 2017). As the error of pNO_3^- formation simulation was subject to the ClNO_2 yield, a higher yield would increase the model uncertainty directly, hence probing the ClNO_2 yield is warranted in future studies. As for NO_3 reactivity, Fig. 7 shows the sensitivity tests of the integral pNO_3^- formation for the whole night at k_{NO_3} values = 0.001 s^{-1} , 0.01 s^{-1} , 0.02 s^{-1} , and 0.05 s^{-1} . The integral pNO_3^- formation decreased when k_{NO_3} varied from 0.001 s^{-1} to 0.1 s^{-1} , but the variation ratio to the base case was within

±5%. The result shows the NO₃-N₂O₅ loss via NO₃ reaction with VOCs during the polluted wintertime was not important, which may only lead to relatively small uncertainties in the integral pNO₃⁻ formation calculation. Nevertheless, if N₂O₅ uptake was extremely low (e.g., $\gamma_{\text{N}_2\text{O}_5} < 10^{-4}$), the uncertainty of NO₃ oxidation would increase significantly.

4. Conclusion

During the wintertime, ambient O₃ is often fully titrated at the ground level in urban Beijing owing to its fast reaction with NO emissions. Consequently, the near-surface air masses are chemically inert. Nevertheless, the chemical information of the air masses at higher altitudes was indicative of a reactive layer above urban Beijing, which potentially drives fast pNO₃⁻ production via N₂O₅ uptake and contributes to the surface PM mass concentration. In this study, we evidenced additional O_x missing (25 ppbv) aloft throughout the night. Based on model simulation, we found that the particulate nitrate formed above 150 m reached 50 µg m⁻³ and enhanced the surface level PM concentration significantly by 28 µg m⁻³ with downward mixing after break-up of the NBL in the morning. Our study also demonstrated that during the heavy PM pollution period, the particulate nitrate formation capacity via N₂O₅ uptake was easily maximized in the upper layer, even with N₂O₅ uptake as low as 2×10⁻³. This indicates that the mixing ratio of NO₂ aloft was directly linked to nitrate formation, and reduction of NO_x is helpful in decreasing nocturnal nitrate formation. Overall, this study highlights the importance of the interplay between chemical formation aloft and dynamic processes for probing the ground-level PM pollution problem. In the future, direct observations of N₂O₅ and associated parameters should be performed to explore the physical and chemical properties of this overhead nighttime reaction layer and to reach a better understanding of the winter haze formation.

432 ***Acknowledgements.***

433 This work was supported by the National Natural Science Foundation of China (Grant
434 No. 91544225, 41375124, 21522701, 41571130021), the National Key Technology
435 Research and Development Program of the Ministry of Science and Technology of
436 China (Grant No. 2014BAC21B01). The authors gratefully acknowledge the science
437 team of Peking University for their general support, as well as the team running the
438 tower platform, which enabled the vertical profile observations.

References.

- Baasandorj, M., Hoch, S. W., Bares, R., Lin, J. C., Brown, S. S., Millet, D. B., Martin, R., Kelly, K., Zarzana, K. J., Whiteman, C. D., Dube, W. P., Tonnesen, G., Jaramillo, I. C., and Sohl, J.: Coupling between Chemical and Meteorological Processes under Persistent Cold-Air Pool Conditions: Evolution of Wintertime PM_{2.5} Pollution Events and N₂O₅ Observations in Utah's Salt Lake Valley, *Environ Sci Technol*, 51, 5941-5950, 2017.
- Badger, C. L., Griffiths, P. T., George, I., Abbatt, J. P. D., and Cox, R. A.: Reactive uptake of N₂O₅ by aerosol particles containing mixtures of humic acid and ammonium sulfate, *J Phys Chem A*, 110, 6986-6994, 2006.
- Benton, A. K., Langridge, J. M., Ball, S. M., Bloss, W. J., Dall'Osto, M., Nemitz, E., Harrison, R. M., and Jones, R. L.: Night-time chemistry above London: measurements of NO₃ and N₂O₅ from the BT Tower, *Atmos Chem Phys*, 10, 9781-9795, 2010.
- Bertram, T. H., Thornton, J. A., and Riedel, T. P.: An experimental technique for the direct measurement of N₂O₅ reactivity on ambient particles, *Atmos Meas Tech*, 2, 231-242, 2009.
- Birks, J. W., Andersen, P. C., Williford, C. J., Turnipseed, A. A., Strunk, S. E., Ennis, C. A., and Mattson, E.: Folded Tubular Photometer for atmospheric measurements of NO₂ and NO, *Atmos. Meas. Tech. Discuss.*, <https://doi.org/10.5194/amt-2018-24>, in review, 2018.
- Brown, S. G., Roberts, P. T., McCarthy, M. C., Lurmann, F. W., and Hyslop, N. P.: Wintertime vertical variations in particulate matter (PM) and precursor concentrations in the San Joaquin Valley during the California Regional coarse PM/fine PM Air Quality Study, *J Air Waste Manage*, 56, 1267-1277, 2006.
- Brown, S. S., Dube, W. P., Fuchs, H., Ryerson, T. B., Wollny, A. G., Brock, C. A., Bahreini, R., Middlebrook, A. M., Neuman, J. A., Atlas, E., Roberts, J. M., Osthoff, H. D., Trainer, M., Fehsenfeld, F. C., and Ravishankara, A. R.: Reactive uptake coefficients for N₂O₅ determined from aircraft measurements during the Second Texas Air Quality Study: Comparison to current model parameterizations, *J Geophys Res-Atmos*, 114, 2009.
- Brown, S. S., Dube, W. P., Osthoff, H. D., Wolfe, D. E., Angevine, W. M., and Ravishankara, A. R.: High resolution vertical distributions of NO₃ and N₂O₅ through the nocturnal boundary layer, *Atmos Chem Phys*, 7, 139-149, 2007.
- Brown, S. S., Dube, W. P., Tham, Y. J., Zha, Q. Z., Xue, L. K., Poon, S., Wang, Z., Blake, D. R., Tsui, W., Parrish, D. D., and Wang, T.: Nighttime chemistry at a high altitude site above Hong Kong, *J Geophys Res-Atmos*, 121, 2457-2475, 2016.
- Brown, S. S., Ryerson, T. B., Wollny, A. G., Brock, C. A., Peltier, R., Sullivan, A. P., Weber, R. J., Dube, W. P., Trainer, M., Meagher, J. F., Fehsenfeld, F. C., and Ravishankara, A. R.: Variability in nocturnal nitrogen oxide processing and its role in regional air quality, *Science*, 311, 67-70, 2006.
- Brown, S. S. and Stutz, J.: Nighttime radical observations and chemistry, *Chem Soc Rev*, 41, 6405-6447, 2012.
- Cao, J. J., Xu, H. M., Xu, Q., Chen, B. H., and Kan, H. D.: Fine Particulate Matter Constituents and Cardiopulmonary Mortality in a Heavily Polluted Chinese City, *Environ Health Persp*, 120, 373-378, 2012.
- Chan, C. Y., Xu, X. D., Li, Y. S., Wong, K. H., Ding, G. A., Chan, L. Y., and Cheng, X. H.: Characteristics of vertical profiles and sources of PM_{2.5}, PM₁₀ and carbonaceous species in Beijing, *Atmos Environ*, 39, 5113-5124, 2005.

483 Chang, W. L., Bhawe, P. V., Brown, S. S., Riemer, N., Stutz, J., and Dabdub, D.: Heterogeneous
 484 Atmospheric Chemistry, Ambient Measurements, and Model Calculations of N₂O₅: A
 485 Review, *Aerosol Sci Tech*, 45, 665-695, 10.1080/02786826.2010.551672, 2011.
 486 Chang, W. L., Brown, S. S., Stutz, J., Middlebrook, A. M., Bahreini, R., Wagner, N. L., Dube, W.
 487 P., Pollack, I. B., Ryerson, T. B., and Riemer, N.: Evaluating N₂O₅ heterogeneous hydrolysis
 488 parameterizations for CalNex 2010, *J Geophys Res-Atmos*, 121, 5051-5070,
 489 10.1002/2015jd024737, 2016.
 490 Chen, C., Sun, Y. L., Xu, W. Q., Du, W., Zhou, L. B., Han, T. T., Wang, Q. Q., Fu, P. Q., Wang, Z.
 491 F., Gao, Z. Q., Zhang, Q., and Worsnop, D. R.: Characteristics and sources of submicron
 492 aerosols above the urban canopy (260 m) in Beijing, China, during the 2014 APEC summit,
 493 *Atmos Chem Phys*, 15, 12879-12895, 2015.
 494 Crowley, J. N., Ammann, M., Cox, R. A., Hynes, R. G., Jenkin, M. E., Mellouki, A., Rossi, M. J.,
 495 Troe, J., and Wallington, T. J.: Evaluated kinetic and photochemical data for atmospheric
 496 chemistry: Volume V - heterogeneous reactions on solid substrates, *Atmos Chem Phys*, 10,
 497 9059-9223, 2010b.
 498 Crowley, J. N., Schuster, G., Pouvesle, N., Parchatka, U., Fischer, H., Bonn, B., Bingemer, H., and
 499 Lelieveld, J.: Nocturnal nitrogen oxides at a rural mountain-site in south-western Germany,
 500 *Atmos Chem Phys*, 10, 2795-2812, 2010a.
 501 Ferrero, L., Cappelletti, D., Moroni, B., Sangiorgi, G., Perrone, M. G., Crocchianti, S., and
 502 Bolzacchini, E.: Wintertime aerosol dynamics and chemical composition across the mixing
 503 layer over basin valleys, *Atmos Environ*, 56, 143-153, 2012.
 504 Ferrero, L., Perrone, M. G., Petraccone, S., Sangiorgi, G., Ferrini, B. S., Lo Porto, C., Lazzati, Z.,
 505 Cocchi, D., Bruno, F., Greco, F., Riccio, A., and Bolzacchini, E.: Vertically-resolved particle
 506 size distribution within and above the mixing layer over the Milan metropolitan area, *Atmos*
 507 *Chem Phys*, 10, 3915-3932, 2010.
 508 Geyer, A., and Stutz, J.: Vertical profiles of NO₃, N₂O₅, O₃, and NO_x in the nocturnal boundary
 509 layer: 2. Model studies on the altitude dependence of composition and chemistry, *J Geophys*
 510 *Res-Atmos*, 109, Artn D12307 Doi 10.1029/2003jd004211, 2004.
 511 Green, M. C.; Chow, J. C.; Watson, J. G.; Dick, K.; Inouye, D., Effects of snow cover and
 512 atmospheric stability on winter PM_{2.5} concentrations in Western U.S. valleys. *J. Appl.*
 513 *Meteor. Climatol.* 2015, 54 (6), 1191-1201. DOI 10.1175/JAMC-D-14-0191.1.
 514 Gross, S. and Bertram, A. K.: Reactive uptake of NO₃, N₂O₅, NO₂, HNO₃, and O₃ on three types
 515 of polycyclic aromatic hydrocarbon surfaces, *J Phys Chem A*, 112, 3104-3113, 2008.
 516 Gross, S., Iannone, R., Xiao, S., and Bertram, A. K.: Reactive uptake studies of NO₃ and N₂O₅ on
 517 alkenoic acid, alkanoate, and polyalcohol substrates to probe nighttime aerosol chemistry,
 518 *Phys Chem Chem Phys*, 11, 7792-7803, 2009.
 519 Grzinic, G., Bartels-Rausch, T., Berkemeier, T., Turler, A., and Ammann, M.: Viscosity controls
 520 humidity dependence of N₂O₅ uptake to citric acid aerosol, *Atmos Chem Phys*, 15,
 521 13615-13625, 2015.
 522 Guo, S., Hu, M., Zamora, M. L., Peng, J. F., Shang, D. J., Zheng, J., Du, Z. F., Wu, Z., Shao, M.,
 523 Zeng, L. M., Molina, M. J., and Zhang, R. Y.: Elucidating severe urban haze formation in
 524 China, *P Natl Acad Sci USA*, 111, 17373-17378, 2014.
 525 Hallquist, M., Stewart, D. J., Stephenson, S. K., and Cox, R. A.: Hydrolysis of N₂O₅ on
 526 sub-micron sulfate aerosols, *Phys Chem Chem Phys*, 5, 3453-3463, 2003.

527 Huang, R. J., Zhang, Y. L., Bozzetti, C., Ho, K. F., Cao, J. J., Han, Y. M., Daellenbach, K. R.,
 528 Slowik, J. G., Platt, S. M., Canonaco, F., Zotter, P., Wolf, R., Pieber, S. M., Bruns, E. A.,
 529 Crippa, M., Ciarelli, G., Piazzalunga, A., Schwikowski, M., Abbaszade, G., Schnelle-Kreis, J.,
 530 Zimmermann, R., An, Z. S., Szidat, S., Baltensperger, U., El Haddad, I., and Prevot, A. S. H.:
 531 High secondary aerosol contribution to particulate pollution during haze events in China,
 532 *Nature*, 514, 218-222, 2014.

533 Kane, S. M., Caloz, F., and Leu, M. T.: Heterogeneous uptake of gaseous N_2O_5 by $(\text{NH}_4)_2\text{SO}_4$,
 534 NH_4HSO_4 , and H_2SO_4 aerosols, *J Phys Chem A*, 105, 6465-6470, 2001.

535 Kim, Y. J., Spak, S. N., Carmichael, G. R., Riemer, N., and Stanier, C. O.: Modeled aerosol nitrate
 536 formation pathways during wintertime in the Great Lakes region of North America, *J*
 537 *Geophys Res-Atmos*, 119, 12420-12445, 2014.

538 Lei, H. and Wuebbles, D. J.: Chemical competition in nitrate and sulfate formations and its effect
 539 on air quality, *Atmos Environ*, 80, 472-477, 2013.

540 Lurmann, F. W., Brown, S. G., McCarthy, M. C., and Roberts, P. T.: Processes influencing
 541 secondary aerosol formation in the San Joaquin Valley during winter, *J Air Waste Manage*, 56,
 542 1679-1693, 2006.

543 Mentel, T. F., Sohn, M., and Wahner, A.: Nitrate effect in the heterogeneous hydrolysis of
 544 dinitrogen pentoxide on aqueous aerosols, *Phys Chem Chem Phys*, 1, 5451-5457, 1999.

545 Morgan, W. T., Ouyang, B., Allan, J. D., Aruffo, E., Di Carlo, P., Kennedy, O. J., Lowe, D., Flynn,
 546 M. J., Rosenberg, P. D., Williams, P. I., Jones, R., McFiggans, G. B., and Coe, H.: Influence
 547 of aerosol chemical composition on N_2O_5 uptake: airborne regional measurements in
 548 northwestern Europe, *Atmos Chem Phys*, 15, 973-990, 2015.

549 Pathak, R. K., Wang, T., and Wu, W. S.: Nighttime enhancement of $\text{PM}_{2.5}$ nitrate in ammonia-poor
 550 atmospheric conditions in Beijing and Shanghai: Plausible contributions of heterogeneous
 551 hydrolysis of N_2O_5 and HNO_3 partitioning, *Atmos Environ*, 45, 1183-1191, 2011.

552 Pathak, R. K., Wu, W. S., and Wang, T.: Summertime $\text{PM}_{2.5}$ ionic species in four major cities of
 553 China: nitrate formation in an ammonia-deficient atmosphere, *Atmos Chem Phys*, 9,
 554 1711-1722, 2009.

555 Phillips, G. J., Thieser, J., Tang, M. J., Sobanski, N., Schuster, G., Fachinger, J., Drewnick, F.,
 556 Borrmann, S., Bingemer, H., Lelieveld, J., and Crowley, J. N.: Estimating N_2O_5 uptake
 557 coefficients using ambient measurements of NO_3 , N_2O_5 , ClNO_2 and particle-phase nitrate,
 558 *Atmos Chem Phys*, 16, 13231-13249, 2016.

559 Prabhakar, G., Parworth, C. L., Zhang, X. L., Kim, H., Young, D. E., Beyersdorf, A. J., Ziemba, L.
 560 D., Nowak, J. B., Bertram, T. H., Faloon, I. C., Zhang, Q., and Cappa, C. D.: Observational
 561 assessment of the role of nocturnal residual-layer chemistry in determining daytime surface
 562 particulate nitrate concentrations, *Atmos Chem Phys*, 17, 14747-14770,
 563 10.5194/acp-17-14747-2017, 2017.

564 Pusede, S. E., Duffey, K. C., Shusterman, A. A., Saleh, A., Laughner, J. L., Wooldridge, P. J.,
 565 Zhang, Q., Parworth, C. L., Kim, H., Capps, S. L., Valin, L. C., Cappa, C. D., Fried, A.,
 566 Walega, J., Nowak, J. B., Weinheimer, A. J., Hoff, R. M., Berkoff, T. A., Beyersdorf, A. J.,
 567 Olson, J., Crawford, J. H., and Cohen, R. C.: On the effectiveness of nitrogen oxide
 568 reductions as a control over ammonium nitrate aerosol, *Atmos Chem Phys*, 16, 2575-2596,
 569 2016.

570 Riedel, T. P., Wagner, N. L., Dube, W. P., Middlebrook, A. M., Young, C. J., Ozturk, F., Bahreini,

R., VandenBoer, T. C., Wolfe, D. E., Williams, E. J., Roberts, J. M., Brown, S. S., and Thornton, J. A.: Chlorine activation within urban or power plant plumes: Vertically resolved ClNO_2 and Cl_2 measurements from a tall tower in a polluted continental setting, *J Geophys Res-Atmos*, 118, 8702-8715, 2013.

Sander, S. P., et al. (2011), Chemical Kinetics and Photochemical Data for Use in Atmospheric Studies Evaluation Number 17, JPL Publication 10–6 Rep., NASA Jet Propul. Lab, Pasadena, California.

Seinfeld, J. H., Pandis, S.N., (2006). Atmospheric Chemistry and Physics: from Air Pollution to Climate Change (Second edition), John Wiley & Sons, Inc., Hoboken, New Jersey.

Stutz, J., Alicke, B., Ackermann, R., Geyer, A., White, A., and Williams, E.: Vertical profiles of NO_3 , N_2O_5 , O-3, and NO_x in the nocturnal boundary layer: 1. Observations during the Texas Air Quality Study 2000, *J Geophys Res-Atmos*, 109, Art. D12306 10.1029/2003jd004209, 2004.

Stutz, J., Wong, K. W., Lawrence, L., Ziemba, L., Flynn, J. H., Rappengluck, B., and Lefer, B.: Nocturnal NO_3 radical chemistry in Houston, TX, *Atmos Environ*, 44, 4099-4106, 2010.

Su, X., Tie, X. X., Li, G. H., Cao, J. J., Huang, R. J., Feng, T., Long, X., and Xu, R. G.: Effect of hydrolysis of N_2O_5 on nitrate and ammonium formation in Beijing China: WRF-Chem model simulation, *Sci Total Environ*, 579, 221-229, 2017.

Sun, Y. L., Du, W., Wan, Q. Q., Zhang, Q., Chen, C., Chen, Y., Chen, Z. Y., Fu, P. Q., Wang, Z. F., Gao, Z. Q., and Worsnop, D. R.: Real-Time Characterization of Aerosol Particle Composition above the Urban Canopy in Beijing: Insights into the Interactions between the Atmospheric Boundary Layer and Aerosol Chemistry, *Environ Sci Technol*, 49, 11340-11347, 2015b.

Sun, Y. L., Wang, Z. F., Du, W., Zhang, Q., Wang, Q. Q., Fu, P. Q., Pan, X. L., Li, J., Jayne, J., and Worsnop, D. R.: Long-term real-time measurements of aerosol particle composition in Beijing, China: seasonal variations, meteorological effects, and source analysis, *Atmos Chem Phys*, 15, 10149-10165, 2015a.

Sun, Y. L., Wang, Z. F., Fu, P. Q., Yang, T., Jiang, Q., Dong, H. B., Li, J., and Jia, J. J.: Aerosol composition, sources and processes during wintertime in Beijing, China, *Atmos Chem Phys*, 13, 4577-4592, 2013.

Tham, Y. J., Wang, Z., Li, Q. Y., Yun, H., Wang, W. H., Wang, X. F., Xue, L. K., Lu, K. D., Ma, N., Bohn, B., Li, X., Kecorius, S., Gross, J., Shao, M., Wiedensohler, A., Zhang, Y. H., and Wang, T.: Significant concentrations of nitryl chloride sustained in the morning: investigations of the causes and impacts on ozone production in a polluted region of northern China, *Atmos Chem Phys*, 16, 14959-14977, 2016.

Thornton, J. A., Braban, C. F., and Abbatt, J. P. D.: N_2O_5 hydrolysis on sub-micron organic aerosols: the effect of relative humidity, particle phase, and particle size, *Phys Chem Chem Phys*, 5, 4593-4603, 2003.

Thornton, J. A., Kercher, J. P., Riedel, T. P., Wagner, N. L., Cozic, J., Holloway, J. S., Dube, W. P., Wolfe, G. M., Quinn, P. K., Middlebrook, A. M., Alexander, B., and Brown, S. S.: A large atomic chlorine source inferred from mid-continental reactive nitrogen chemistry, *Nature*, 464, 271-274, 2010.

Tsai, C., Wong, C., Hurlock, S., Pikelnaya, O., Mielke, L. H., Osthoff, H. D., Flynn, J. H., Haman, C., Lefer, B., Gilman, J., de Gouw, J., and Stutz, J.: Nocturnal loss of NO_x during the 2010 CalNex-LA study in the Los Angeles Basin, *J Geophys Res-Atmos*, 119, 13004-13025, 2014.

- Wagner, N. L., Riedel, T. P., Young, C. J., Bahreini, R., Brock, C. A., Dube, W. P., Kim, S., Middlebrook, A. M., Ozturk, F., Roberts, J. M., Russo, R., Sive, B., Swarthout, R., Thornton, J. A., VandenBoer, T. C., Zhou, Y., and Brown, S. S.: N_2O_5 uptake coefficients and nocturnal NO_2 removal rates determined from ambient wintertime measurements, *J Geophys Res-Atmos*, 118, 9331-9350, 2013.
- Wahner, A., Mentel, T. F., and Sohn, M.: Gas-phase reaction of N_2O_5 with water vapor: Importance of heterogeneous hydrolysis of N_2O_5 and surface desorption of HNO_3 in a large teflon chamber, *Geophys Res Lett*, 25, 2169-2172, 1998.
- Wang, G. H., Zhang, R. Y., Gomez, M. E., Yang, L. X., Zamora, M. L., Hu, M., Lin, Y., Peng, J. F., Guo, S., Meng, J. J., Li, J. J., Cheng, C. L., Hu, T. F., Ren, Y. Q., Wang, Y. S., Gao, J., Cao, J. J., An, Z. S., Zhou, W. J., Li, G. H., Wang, J. Y., Tian, P. F., Marrero-Ortiz, W., Secrest, J., Du, Z. F., Zheng, J., Shang, D. J., Zeng, L. M., Shao, M., Wang, W. G., Huang, Y., Wang, Y., Zhu, Y. J., Li, Y. X., Hu, J. X., Pan, B., Cai, L., Cheng, Y. T., Ji, Y. M., Zhang, F., Rosenfeld, D., Liss, P. S., Duce, R. A., Kolb, C. E., and Molina, M. J.: Persistent sulfate formation from London Fog to Chinese haze, *P Natl Acad Sci USA*, 113, 13630-13635, 10.1073/pnas.1616540113, 2016.
- Wang, H. C. and Lu, K. D.: Determination and Parameterization of the Heterogeneous Uptake Coefficient of Dinitrogen Pentoxide (N_2O_5), *Prog Chem*, 28, 917-933, 2016.
- Wang, H. C., Lu, K. D., Chen, X. R., Zhu, Q. D., Chen, Q., Guo, S., Jiang, M. Q., Li, X., Shang, D. J., Tan, Z. F., Wu, Y. S., Wu, Z. J., Zou, Q., Zheng, Y., Zeng, L. M., Zhu, T., Hu, M., and Zhang, Y. H.: High N_2O_5 Concentrations Observed in Urban Beijing: Implications of a Large Nitrate Formation Pathway, *Environ Sci Tech Lett*, 4, 416-420, 2017b.
- Wang, H. C., Lu, K. D., Tan, Z. F., Sun, K., Li, X., Hu, M., Shao, M., Zeng, L. M., Zhu, T., and Zhang, Y. H.: Model simulation of NO_3 , N_2O_5 and ClNO_2 at a rural site in Beijing during CAREBeijing-2006, *Atmos Res*, 196, 97-107, 2017a.
- Wang, H., Lu, K., Guo, S., Wu, Z., Shang, D., Tan, Z., Wang, Y., Le Breton, M., Zhu, W., Lou, S., Tang, M., Wu, Y., Zheng, J., Zeng, L., Hallquist, M., Hu, M., and Zhang, Y.: Efficient N_2O_5 Uptake and NO_3 Oxidation in the Outflow of Urban Beijing, *Atmos. Chem. Phys. Discuss.*, <https://doi.org/10.5194/acp-2018-88>, in review, 2018.
- Wang, X. F., Wang, H., Xue, L. K., Wang, T., Wang, L. W., Gu, R. R., Wang, W. H., Tham, Y. J., Wang, Z., Yang, L. X., Chen, J. M., and Wang, W. X.: Observations of N_2O_5 and ClNO_2 at a polluted urban surface site in North China: High N_2O_5 uptake coefficients and low ClNO_2 product yields, *Atmos Environ*, 156, 125-134, 2017.
- Wang, Z., Wang, W. H., Tham, Y. J., Li, Q. Y., Wang, H., Wen, L., Wang, X. F., and Wang, T.: Fast heterogeneous N_2O_5 uptake and ClNO_2 production in power plant and industrial plumes observed in the nocturnal residual layer over the North China Plain, *Atmos Chem Phys*, 17, 12361-12378, 2017.
- Watson, J. G. and Chow, J. C.: A wintertime $\text{PM}_{2.5}$ episode at the fresno, CA, supersite, *Atmos Environ*, 36, 465-475, 2002.
- Wen, L. A., Chen, J. M., Yang, L. X., Wang, X. F., Xu, C. H., Sui, X. A., Yao, L., Zhu, Y. H., Zhang, J. M., Zhu, T., and Wang, W. X.: Enhanced formation of fine particulate nitrate at a rural site on the North China Plain in summer: The important roles of ammonia and ozone, *Atmos Environ*, 101, 294-302, 2015.
- Ying, Q.: Physical and chemical processes of wintertime secondary nitrate aerosol formation,

659 Front Environ Sci En, 5, 348-361, 2011.

660 Zhang, Q., Jimenez, J. L., Canagaratna, M. R., Allan, J. D., Coe, H., Ulbrich, I., Alfarra, M. R.,
661 Takami, A., Middlebrook, A. M., Sun, Y. L., Dzepina, K., Dunlea, E., Docherty, K., DeCarlo,
662 P. F., Salcedo, D., Onasch, T., Jayne, J. T., Miyoshi, T., Shimojo, A., Hatakeyama, S.,
663 Takegawa, N., Kondo, Y., Schneider, J., Drewnick, F., Borrmann, S., Weimer, S., Demerjian,
664 K., Williams, P., Bower, K., Bahreini, R., Cottrell, L., Griffin, R. J., Rautiainen, J., Sun, J. Y.,
665 Zhang, Y. M., and Worsnop, D. R.: Ubiquity and dominance of oxygenated species in organic
666 aerosols in anthropogenically-influenced Northern Hemisphere midlatitudes, *Geophys Res*
667 *Lett*, 34, 2007.

668 Zhang, R. Y., Wang, G. H., Guo, S., Zarnora, M. L., Ying, Q., Lin, Y., Wang, W. G., Hu, M., and
669 Wang, Y.: Formation of Urban Fine Particulate Matter, *Chem Rev*, 115, 3803-3855, 2015.

670 Zheng, G. J., Duan, F. K., Su, H., Ma, Y. L., Cheng, Y., Zheng, B., Zhang, Q., Huang, T., Kimoto,
671 T., Chang, D., Poschl, U., Cheng, Y. F., and He, K. B.: Exploring the severe winter haze in
672 Beijing: the impact of synoptic weather, regional transport and heterogeneous reactions,
673 *Atmos Chem Phys*, 15, 2969-2983, 2015.

674 Zhong, J. T., Zhang, X. Y., Wang, Y. Q., Sun, J. Y., Zhang, Y. M., Wang, J. Z., Tan, K. Y., Shen,
675 X. J., Che, H. C., Zhang, L., Zhang, Z. X., Qi, X. F., Zhao, H. R., Ren, S. X., and Li, Y.:
676 Relative Contributions of Boundary-Layer Meteorological Factors to the Explosive Growth
677 of PM_{2.5} during the Red-Alert Heavy Pollution Episodes in Beijing in December 2016, *J*
678 *Meteorol Res-Prc*, 31, 809-819, 2017.

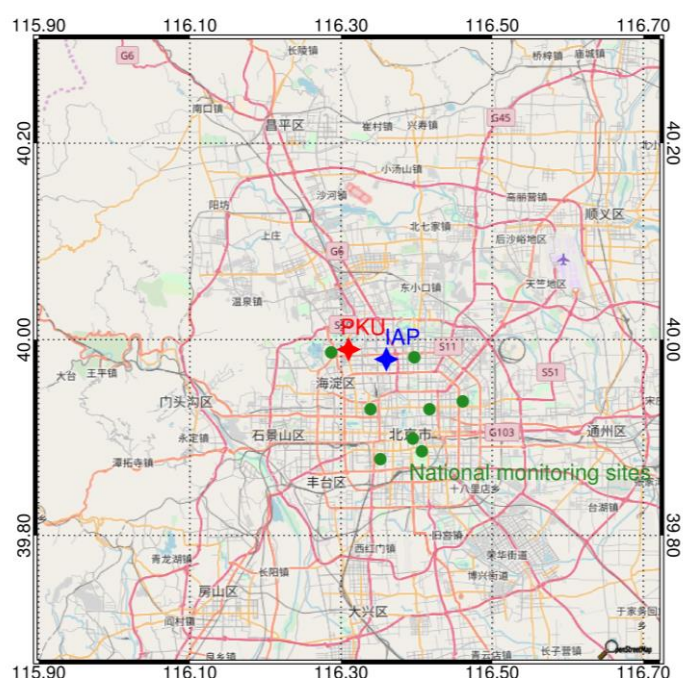


Figure 1. Location of the monitoring sites used in this study, including PKU (red diamond), IAP (blue diamond), and other National Monitoring Sites (green circles). Vertical profiles of NO_x and O_3 were collected at a tower at the IAP. Measurements of particle number and size distribution (used to calculate N_2O_5 and particle nitrate formation) were collected from a ground site at PKU. Additional measurements on $\text{PM}_{2.5}$ concentrations were continuously measured at national monitoring sites throughout Beijing.

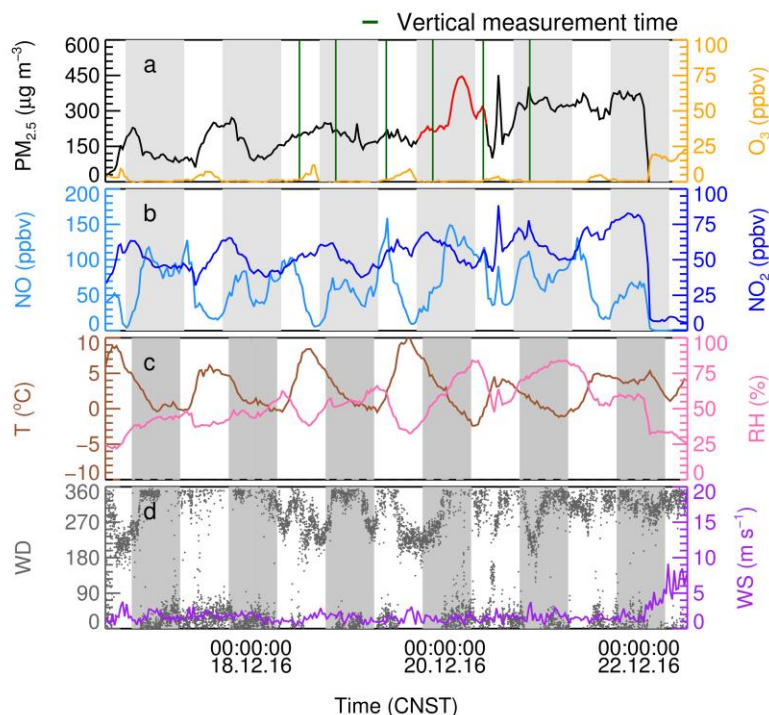


Figure 2. Time series of (a) $\text{PM}_{2.5}$ and O_3 , (b) NO and NO_2 , (c) temperature (T) and relative humidity (RH), (d) wind direction (WD) and wind speed (WS) from December 16 to 22, 2016 at PKU site in Beijing, China. The shaded region represents the nighttime periods. Red line in panel (a) shows an example of fast $\text{PM}_{2.5}$ enhancement on the night of December 19, and the green lines are the time periods when the vertical measurements conducted in IAP site.

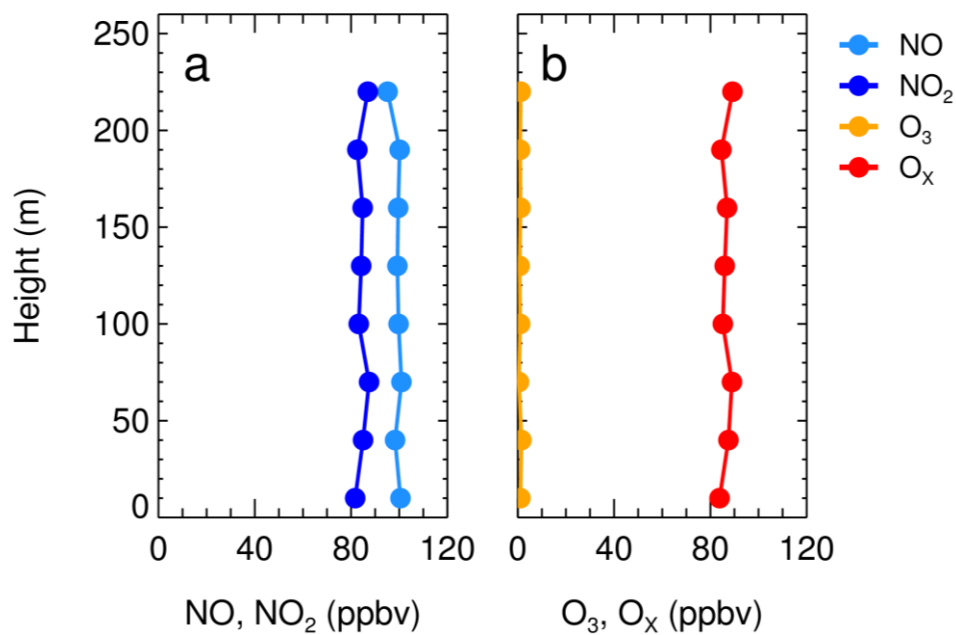


Figure 3. Vertical profiles of NO and NO₂ (a), O₃ and O_x (b) at 20:38-21:06 on the night of December 20, 2016.

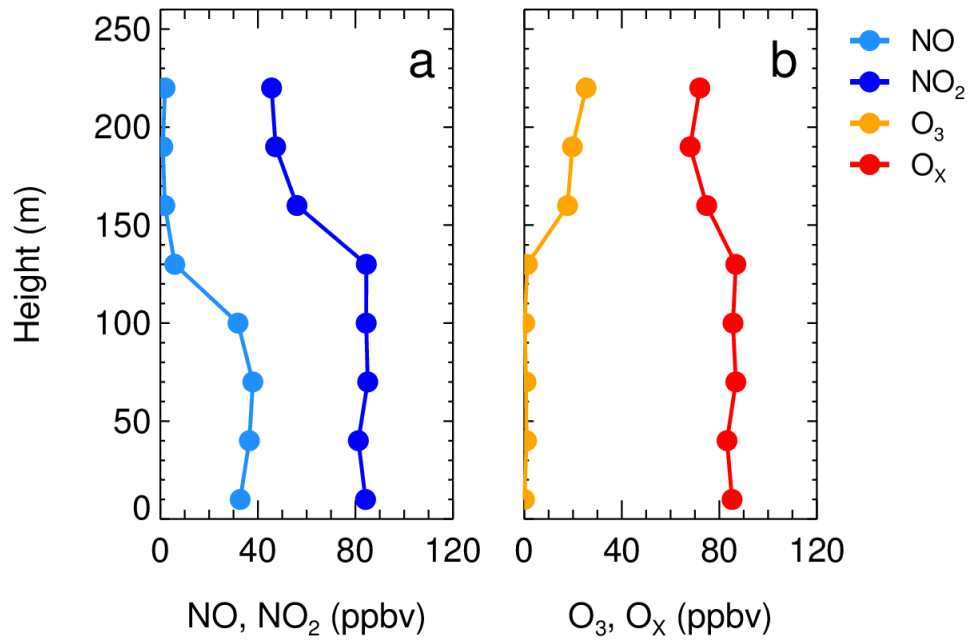


Figure 4. O_x missing case presented by the vertical profiles of (a) NO and NO₂, (b) O₃ and O_x at 20:38-21:13 on the night of December 19, 2016.

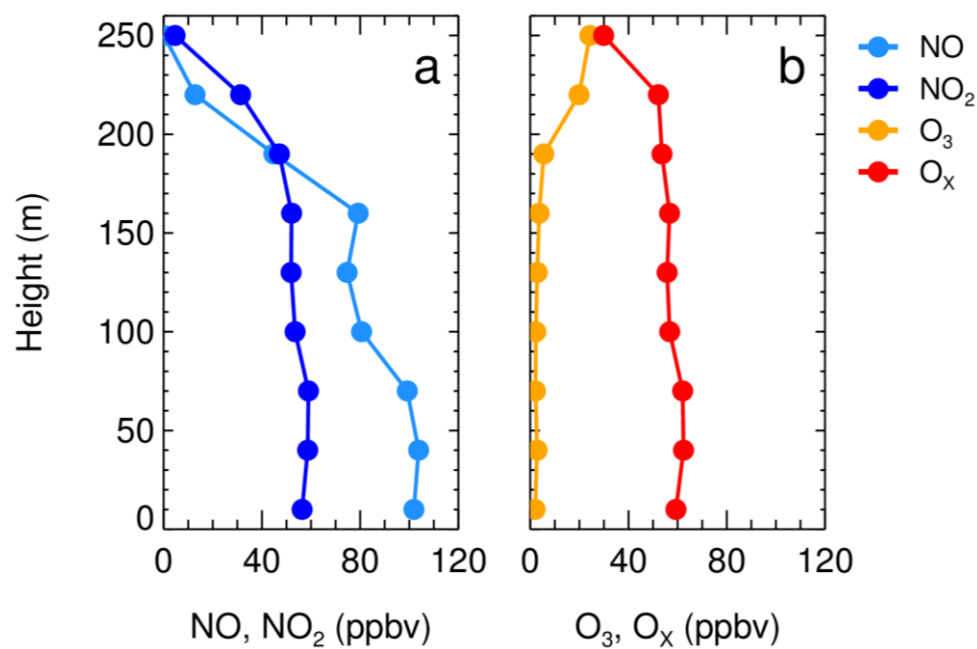


Figure 5. Vertical profiles of (a) NO and NO₂, (b) O₃ and O_x at 09:06-09:34 in the morning of December 20, 2016.

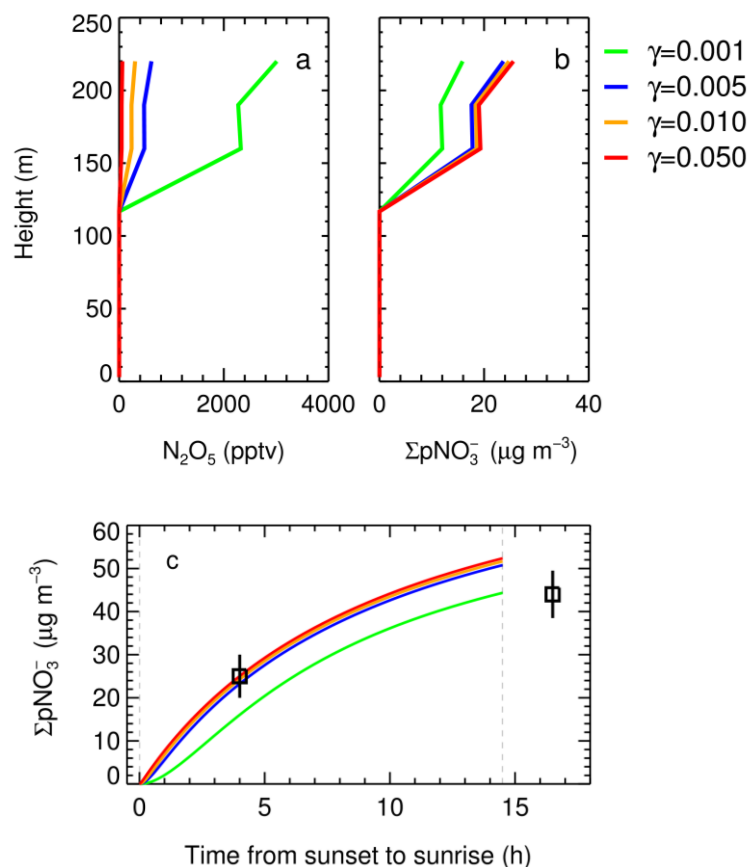


Figure 6. Base case ($\gamma=0.005$) and sensitivity tests of the vertical profile on the night of December 19 at different N_2O_5 uptake coefficients, including (a) the mixing ratio of N_2O_5 at 21:00, (b) the integral pNO_3^- production from sunset to 21:00, (c) the time series of the integral pNO_3^- formed at 240 m via N_2O_5 uptake from sunset (17:00) to sunrise (07:30, nighttime length = 14.5 h), the squares represents the pNO_3^- equivalent weight from the observed O_x missing in the two vertical measurements ~21:00 and ~09:30 in the following morning.

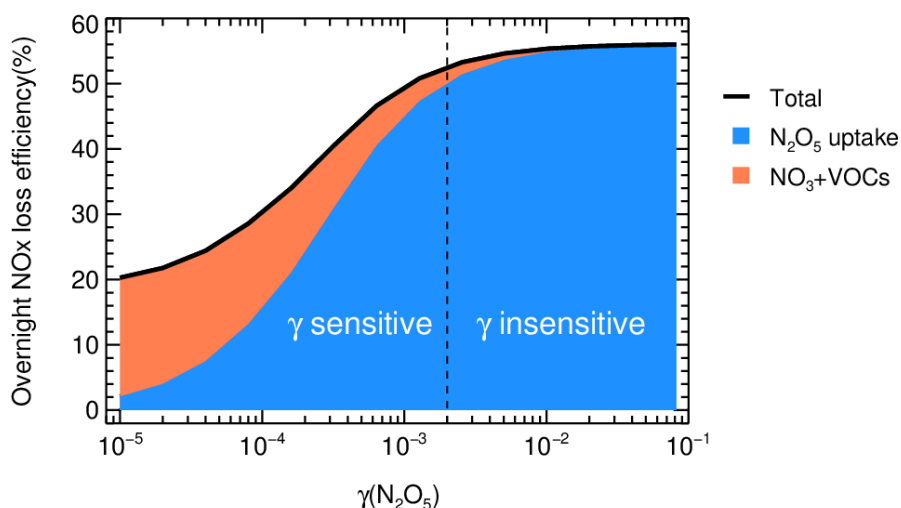


Figure 7. The dependence of overnight NO_x loss on N_2O_5 uptake on $\gamma_{\text{N}_2\text{O}_5}$ in a typical winter pollution condition. The initial NO_2 and O_3 set to 60 ppbv and 30 ppbv, respectively, S_a set to $3000 \mu\text{m}^2 \text{cm}^{-3}$, the ClNO_2 yield is zero and k_{NO_3} is 0.02 s^{-1} . The reaction time set to 14.5 h. The blue and orange zone represent the contribution by NO_3+VOCs and N_2O_5 uptake, the dashed line ($\gamma = 0.002$, when N_2O_5 uptake contribute to 90% of the maximum NO_x loss) divide the loss into γ sensitive and insensitive region. The maximum nocturnal NO_x loss by $\text{NO}_3\text{-N}_2\text{O}_5$ chemistry is 56%.

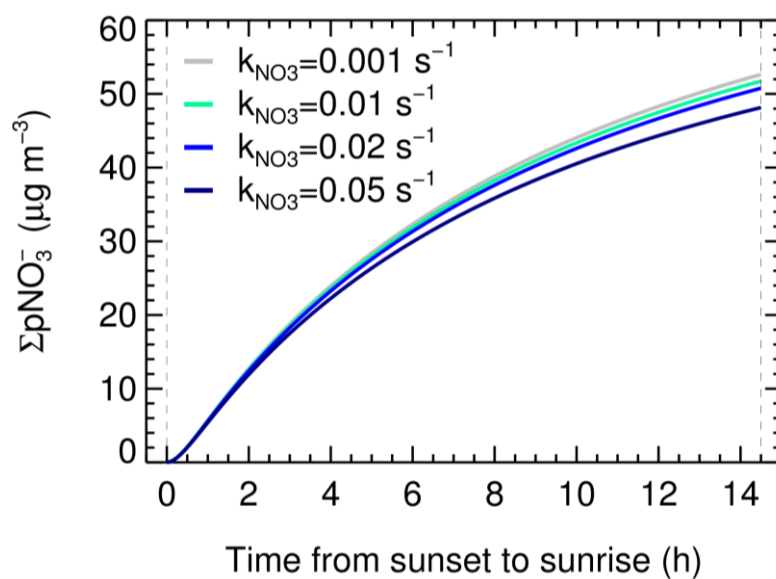


Figure 8. Base case ($k_{\text{NO}_3}=0.02 \text{ s}^{-1}$) and sensitivity tests of the integral pNO_3^- formed at 240 m via N_2O_5 uptake at different NO_3 reactivity (0.001 s^{-1} , 0.01 s^{-1} , 0.05 s^{-1}) on the whole night of December 19, 2016.

731

Table 1. List of the parameter sets in base case and sensitivity tests.

Cases	k_{NO_3} (s^{-1})	$\gamma_{\text{N}_2\text{O}_5}$
Base case	0.02	0.005
k_{NO_3} test 1	0.001	0.005
k_{NO_3} test 2	0.01	0.005
k_{NO_3} test 3	0.05	0.005
$\gamma_{\text{N}_2\text{O}_5}$ test 1	0.02	0.001
$\gamma_{\text{N}_2\text{O}_5}$ test 2	0.02	0.01
$\gamma_{\text{N}_2\text{O}_5}$ test 3	0.02	0.05

732